

Faster Gradient-based NAS Pipeline Combining Broad Scalable Architecture with Confident Learning Rate

Zixiang Ding^{1,2}, Yaran Chen^{1,2}, Nannan Li^{1,2}, Dongbin Zhao^{1,2}

¹ State Key Laboratory of Management and Control for Complex Systems, Institute of Automation
Chinese Academy of Sciences
Beijing 100190, China

² University of Chinese Academy of Sciences
Beijing, 100049 China

{dingzixiang2018, chenyanran2013, linannan2017, dongbin.zhao}@ia.ac.cn

Abstract

In order to further improve the search efficiency of Neural Architecture Search (NAS), we propose B-DARTS, a novel pipeline combining broad scalable architecture with Confident Learning Rate (CLR). In B-DARTS, Broad Convolutional Neural Network (BCNN) is employed as the scalable architecture for DARTS, a popular differentiable NAS approach. On one hand, BCNN is a broad scalable architecture whose topology achieves two advantages compared with the deep one, mainly including faster single-step training speed and higher memory efficiency (i.e. larger batch size for architecture search), which are all contributed to the search efficiency improvement of NAS. On the other hand, DARTS discovers the optimal architecture by gradient-based optimization algorithm, which benefits from two superiorities of BCNN simultaneously. Similar to vanilla DARTS, B-DARTS also suffers from the performance collapse issue, where those weight-free operations are prone to be selected by the search strategy. Therefore, we propose CLR, that considers the confidence of gradient for architecture weights update increasing with the training time of over-parameterized model, to mitigate the above issue. Experimental results on CIFAR-10 and ImageNet show that 1) B-DARTS delivers state-of-the-art efficiency of 0.09 GPU day using first order approximation on CIFAR-10; 2) the learned architecture by B-DARTS achieves competitive performance using state-of-the-art composite multiply-accumulate operations and parameters on ImageNet; and 3) the proposed CLR is effective for performance collapse issue alleviation of both B-DARTS and DARTS.

1 Introduction

NAS has achieved unprecedented accomplishments in the structure design engineering field. However, it needs enormous computational requirements, e.g. more than 20000 GPU days for vanilla NAS (Zoph and Le 2017). The time consuming issue is mitigated by cell, a micro search space proposed in NASNet (Zoph et al. 2018). Currently, most of NAS approaches (Pham et al. 2018; Liu et al. 2018b; Chen et al. 2019; Xie et al. 2018; Liang et al. 2019; Xu et al. 2019) are cell-based, where two types of cells (i.e. normal and reduction cells) are treated as the building blocks of a deep scalable architecture. However, the above deep scalable architecture is time-consuming for both phases of architecture

search and evaluation, due to slow single-step training speed and inefficient memory when using multiple cells.

A broad scalable architecture dubbed BCNN is proposed in BNAS (Ding et al. 2020) to solve the above issue. Different from previous deep scalable architecture, BCNN can use few cells to deliver competitive performance with broad topology. There are two merits of broad topology compared with the deep one, 1) faster single-step training speed and 2) higher memory efficiency (i.e. architecture search with more training data in a mini-batch), that are all conducive to the efficiency improvement of NAS. To discover high-performance BCNN, BNAS employs the combination of Reinforcement Learning (RL) (Williams 1992) and parameters sharing (Pham et al. 2018) which suffers from the unbalanced sampling issue, i.e. unfair training issue (Chu et al. 2019). As a result, only the first virtue of BCNN plays a role in BNAS, due to large batch size makes the unbalanced sampling issue worse.

BCNN is appropriate for almost all of cell-based NAS frameworks using various optimization strategies, e.g. RL (Pham et al. 2018), gradient-based (Liu et al. 2018b; Chen et al. 2019; Xie et al. 2018; Liang et al. 2019; Xu et al. 2019) and Evolutionary Algorithm (EA) (Real et al. 2019). Particularly, gradient-based optimization strategy benefits from the memory efficiency of BCNN greatly, which contributes to the efficiency improvement and uncertainty reduction for architecture search simultaneously (Xu et al. 2019). In this paper, we propose B-DARTS to improve the search efficiency of NAS further. B-DARTS is the combination of broad scalable architecture and a popular gradient-based NAS pipeline, DARTS (Liu et al. 2018b), which benefits from two advantages of BCNN simultaneously. Moreover, B-DARTS delivers terrible performance in terms of accuracy, due to broad topology makes the performance collapse issue (Liang et al. 2019; Xu et al. 2019) worse where more weight-free operations are preferred by the gradient-based search algorithm than vanilla DARTS. Inspired by PC-DARTS (Xu et al. 2019) that uses warmup to mitigate the performance collapse issue, we propose Confident Learning Rate (CLR) that considers the confidence of gradient for architecture weights update increasing with the training time of over-parameterized model. Experimental results on CIFAR-10 and ImageNet show that 1) B-DARTS achieves

5x (state-of-the-art efficiency of 0.09 GPU day) and 7.9x (0.19 GPU day) faster search speed than vanilla DARTS on CIFAR-10 using first and second orders approximation, respectively; 2) the architectures learned by B-DARTS also deliver competitive even better performance than vanilla DARTS; 3) B-DARTS obtains competitive performance using state-of-the-art composite multiply-accumulate operations or parameters on ImageNet; and 4) the proposed CLR is not only effective to mitigate the performance collapse issue in B-DARTS, but also vanilla DARTS.

2 Related Work

Hand-crafted neural networks (e.g. ResNet (He et al. 2016), GoogleNet (Szegedy et al. 2015)) played a predominant role in solving computer vision (Zhao et al. 2017; Chen et al. 2018b), natural language processing (Vaswani et al. 2017) and other artificial intelligence related tasks (Li et al. 2020; Shao et al. 2018, 2019) before NAS (Zoph and Le 2017) was proposed. Recent years, NAS achieved unprecedented success in various tasks, e.g. image classification (Zoph et al. 2018; Pham et al. 2018; Liu et al. 2018b; Chen et al. 2020), semantic segmentation (Liu et al. 2019).

Vanilla NAS (Zoph and Le 2017) greatly suffered from the issue of time consuming. NASNet (Zoph et al. 2018) was proposed to address the above issue, where a micro search space named cell was used to reduce the computational requirements in architecture search phase. Subsequently, lots of cell-based NAS approaches were proposed to further improve the efficiency of NAS, e.g. RL-based ENAS (Pham et al. 2018), gradient-based DARTS (Liu et al. 2018b) and a series of variants of DARTS (e.g. SNAS (Xie et al. 2018), P-DARTS (Chen et al. 2019), PC-DARTS (Xu et al. 2019)). DARTS transferred the NAS problem from discrete space to continuous one, and employed gradient-based algorithm to optimize the architecture weights. Furthermore, PC-DARTS adopted a policy named partial channel connections to realize memory-efficient DARTS.

Beyond that, a broad scalable architecture dubbed BCNN was proposed in RL-based BNAS (Ding et al. 2020). Inspired by Broad Learning System (BLS) (Chen and Liu 2017; Chen et al. 2018a; Feng and Chen 2018), BCNN employed broad (i.e. shallow) topology to obtain faster single-step training speed and higher memory efficiency than the deep one. Moreover, two variants named BNAS-CCE and BNAS-CLE with different broad topology were also proposed for performance promotion. Compared with ENAS (Pham et al. 2018), BNAS delivered 2x less computation cost, 0.2 GPU day that ranked the best in RL-based NAS pipelines. However, only the advantage of fast single-step training speed contributed to the efficiency improvement of BNAS, due to high memory efficiency (i.e. large batch size) aggravated the unbalanced sampling issue (i.e. unfair training issue (Chu et al. 2019)) of large model.

3 Methodology

An overview of B-DARTS is shown in Figure 1. Furthermore, we also introduce three components of B-DARTS, i.e.

gradient-based architecture search pipeline, broad scalable architecture and confident learning rate, in details as below.

3.1 Gradient-based Architecture Search Pipeline

For gradient-based NAS pipeline, an over-parameterized model is constructed by stacking multiple cells following the previous deep topology. Each cell is a directed acyclic graph containing N nodes: 2 input nodes $\{x_{(0)}, x_{(1)}\}$, $N-3$ intermediate nodes $\{x_{(2)}, \dots, x_{(N-2)}\}$, and a single output node $x_{(N-1)}$. Each intermediate node $x_{(i)}$ is a set of feature maps obtained by some operations $o_{(i,j)}(\cdot)$, which are chosen from a predefined search space \mathcal{O} consisting of multiple candidate operations (e.g. convolution, pooling) and used to transform $x_{(j)}$. Hence, each intermediate node can be represented by

$$x_{(i)} = \sum_{j < i} o_{(i,j)}(x_{(j)}). \quad (1)$$

The output of cell is obtained by concatenating the outputs of all intermediate nodes. Subsequently, the core idea of gradient-based NAS pipeline named as continuous relaxation can be expressed by

$$f_{(i,j)}(x_{(j)}) = \sum_{o \in \mathcal{O}} \frac{\exp(\alpha_{(i,j)}^o)}{\sum_{o' \in \mathcal{O}} \exp(\alpha_{(i,j)}^{o'})} o(x_{(j)}), \quad (2)$$

where, operation $o(x_{(j)})$ for a pair of nodes (i, j) is weighted by a hyper-parameter $\alpha_{(i,j)}^o$ of dimension $|\mathcal{O}|$. After continuous relaxation, the NAS pipeline becomes differentiable so that gradient-based algorithm can be employed for parameter optimization. In this paper, we denote α as architecture weights, and the parameters of operations w as network weights.

3.2 Broad Scalable Architecture

As shown in the right side of Figure 1, the broad scalable architecture consists of two components, u convolution blocks where each one contains k deep cells and a single broad cell, and v enhancement blocks where each one includes a single enhancement cell. On one hand, the role of convolution block is similar to feature node played in BLS, i.e. extracting mapped features from input images. Moreover, the functions of deep and broad cells are similar to the normal and reduction cells, for feature extraction and receptive field amplification, respectively. Differently, two types of cells in convolution block are identical with the exception of stride on each operation, where 1 and 2 are set for the deep and broad cells, respectively. On the other hand, the enhancement block is used to enhance the mapped features from convolution blocks through enhancement cell. Moreover, the topology of enhancement cell is different from the convolutional one, and its stride is 1. Based on the above description, we conclude that 1) u is relevant to the size of input fed into the first convolution block, that is similar to the number of reduction cell in previous deep scalable architecture, and 2) k and v are not deterministic as the number of normal cell.

Broad scalable architecture can achieve satisfactory performance using less cells than the deep one, where the combination of multi-scale feature fusion and prior knowledge

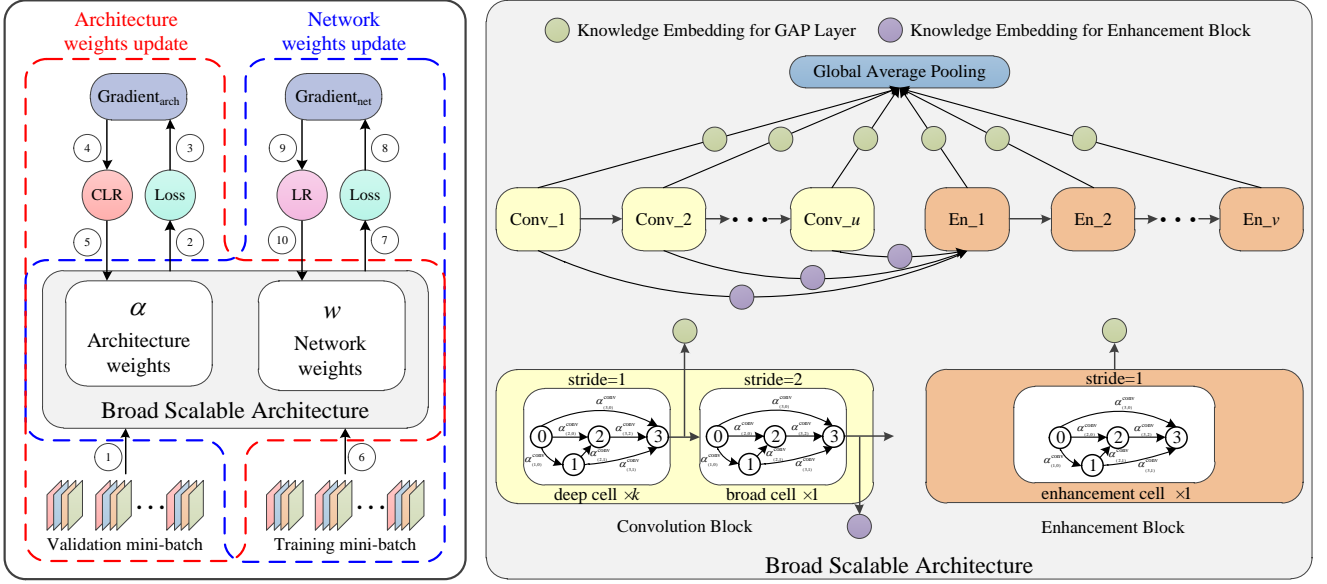


Figure 1: An overview of B-DARTS. For architecture search, there is a loop as below. 1) Architecture weights update: An validation mini-batch is fed into the broad scalable architecture, to obtain the loss for computing the gradient with respect to architecture weights. The proposed CLR is applied to control the gradient confidence. 2) Network weights update: A train mini-batch is treated as the input of broad scalable architecture. Subsequently, the loss is obtained and the gradient with regard to network weights is computed. Finally, the product of gradient and learning rate is employed for network weights update.

imbedding plays an important role. As shown in Figure 1, the Global Average Pooling (GAP) layer does not only treat the high-level representations (i.e. the output of each enhancement block) as input, but also the outputs of each convolution block whose representations are low-level with small receptive field. Those multi-scale features are fused by the GAP layer to yield more comprehensive and effective latent representations for accurate classification. Moreover, the inputs of GAP layer from convolution blocks are the inputs of every broad cell, for obtaining latent representations with full scales. And the output of each broad cell is fed into the first enhancement block for enhancing mapped features. Beyond that, a prior knowledge can be obtained through considerable experiments, that low-level feature contributes to the performance improvement of BCNN if it accounts for few significance. Therefore, each connection with respect to the GAP layer and first enhancement block, is equipped with a knowledge embedding for significance control. Typically, 1×1 convolution where the number of output channels is half of the input, is employed as the knowledge embedding to restrict the significance of low-level latent representations. There are two special knowledge embedding modules whose input and output channels are identical, one on the connection of the last convolution block and the first enhancement block, and another on the connection between the last enhancement block and the GAP layer.

Benefit from two properties, 1) identical topologies of deep and broad cells, and 2) using broad topology to achieve high performance, k and v can be set to 0 and 1 in the architecture search phase for broad scalable architecture based NAS approaches, respectively. There are two advantages us-

ing the above setting, fast single-step training speed and high memory efficiency, that both contribute to the efficiency improvement of NAS. Due to two reasons as below:

- The advantage of memory efficiency dose not always contribute to the accuracy improvement of NAS. Memory efficiency means large batch size can be set in each iteration for architecture search, while making the unbalanced sampling issue (Chu et al. 2019) of large model in some NAS approaches worse, e.g. BNAS (Ding et al. 2020);
- Gradient-based NAS pipeline benefits from memory efficiency. More training data contributes to uncertainty reduction for updating parameters of both network and architecture, as discussed in PC-DARTS (Xu et al. 2019),

we propose B-DARTS, the combination of broad scalable architecture and gradient-based NAS pipeline, to take full advantages of BCNN.

3.3 Confident Learning Rate

In B-DARTS, the performance collapse issue gets worse than vanilla DARTS, where those weight-free operations (e.g. pooling, skip connection) are prone to be selected in both convolution and enhancement cells, especially for the later one (Liang et al. 2019; Xu et al. 2019). To solve this issue, some strategies are proposed, e.g. early stopping (Liang et al. 2019; Liu et al. 2019; Chen et al. 2019), the combination of warmup and partial channel connections (Xu et al. 2019). The above techniques are effective for performance collapse issue alleviation, but resulting in unfair comparison between the search efficiency of B-DARTS and DARTS.

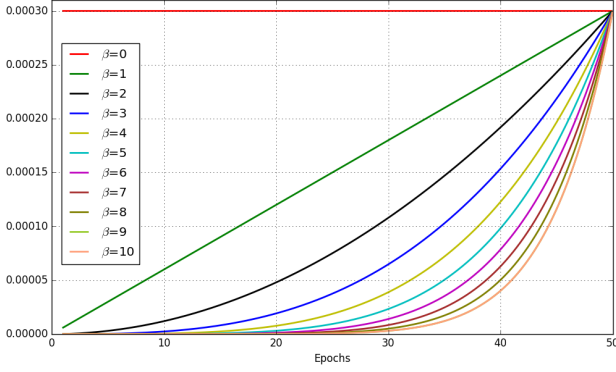


Figure 2: The curves of CLR for B-DARTS and DARTS under various confidence factors. Default architecture learning rate of DARTS is 0.0003.

Therefore, it is important to propose a strategy for solving the above issues simultaneously.

Compared with those weight-equipped operations (e.g. convolution), weight-free operations tend to obtain larger weights before the weights of over-parameterized model are well optimized (Xu et al. 2019). In other words, the confidence of gradient obtained from over-parameterized model should increase with the training time for architecture weights update, so that CLR with respect to the number of current epoch is proposed as

$$lr_{conf}(t) = \left(\frac{t}{T}\right)^\beta \times lr_{arch}, \quad (3)$$

where, t denotes the current epoch from 1 to the maximum T , β represents the confidence factor whose value is directly proportional to the confidence of early over-parameterized model, and lr_{arch} is the initial learning rate for architecture weights. For intuitive comprehension, we plot the curves of CLR under different confidence factors in Figure 2.

How to determine the value of confidence factor β is an intractable problem. With β increasing, more epochs of early training process are involved to freeze the architecture weights, similar to the strategy of warmup used in PC-DARTS (i.e. training architecture weights after 15 epochs). Warmup shows its effectiveness for B-DARTS, so that we make a criterion for β determination as follows.

Criterion 1 *The optimal confidence factor should make the architecture weights starting to be updated at about 15-th epoch.*

4 Experiments and Results

4.1 Datasets and Implementation Details

Similar to DARTS, CIFAR-10 (Krizhevsky and Hinton 2009) and ImageNet (Russakovsky et al. 2015) are also selected for performance evaluation of B-DARTS, with respect to small and large scale image classification tasks, respectively. More details about datasets can be found in **Supplementary Material**.

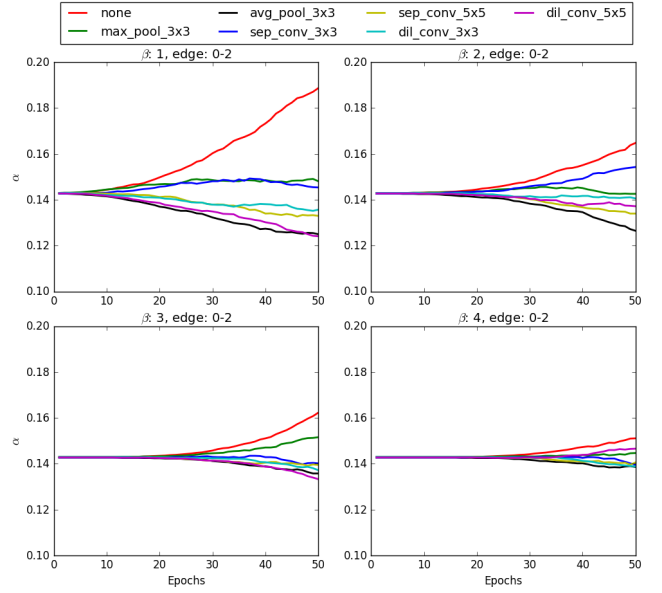


Figure 3: The architecture weights of each operation on the shallowest edge under various confidence factors.

In previous works, search space \mathcal{O} consists of 8 operations, i.e. *separable convolution* with 3×3 and 5×5 kernels, *dilated separable convolution* with 3×3 and 5×5 kernels, *max pooling* and *average pooling* with 3×3 kernel, *skip connection*, and *zero (none)*. In this paper, we remove the *skip connection* from \mathcal{O} for B-DARTS, due to CLR can alleviate the collapse issue in convolution cell rather than enhancement cell. Moreover, *skip connection* will be equipped with largest weight for all edges of enhancement cell, if it is not removed from \mathcal{O} . We show the details of removing *skip connection* in **Supplementary Material**.

4.2 Confidence Factor Determination

In order to find optimal β under **Criterion 1**, we set it from 1 to 4 for architecture search using both B-DARTS and DARTS. The architecture weights α of shallowest edge (connecting the first input node $x_{(0)}$ and the first intermediate node $x_{(2)}$) is chosen as the index for confidence factor determination. We show the experimental results of B-DARTS in Figure 3.

For the first case of B-DARTS, α starts to be updated before 10-th epoch. For $\beta = 3$ and $\beta = 4$, the starting epochs of weights update are both larger than 20. The case of $\beta = 2$ satisfies the **Criterion 1**, i.e. starting to train architecture weights from about 15-th epoch. Consequently, β is set to 2 for next experiments with regard to B-DARTS. Furthermore, we find an interesting phenomenon from Figure 3, that the *none* operation (i.e. red line) always achieves the largest weight when using various confidence factors. The above phenomenon indicates that the proposed CLR does only modify the tendency of weight-equipped operations in later training epochs, rather than imposing small architecture weight on weight-free operations in early training phase. Different from B-DARTS, we set the confidence factor β

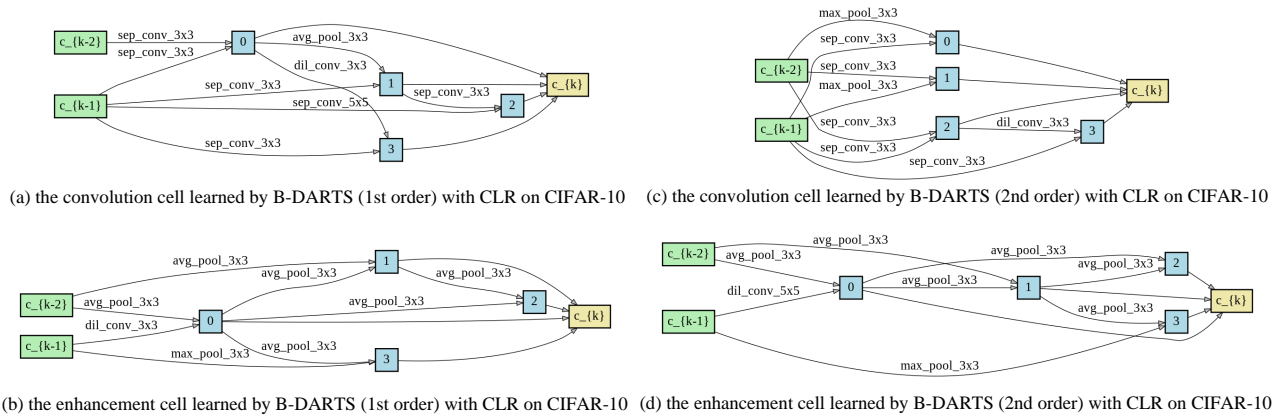


Figure 4: The architectures learned by B-DARTS with CLR using different approximation orders.

Table 1: Comparison of the proposed B-DARTS with CLR and vanilla DARTS on CIFAR-10.

Architecture	Error (%)	Params (M)	Search Cost (GPU days)	Number of Cells	Topology
DARTS (1st order) (Liu et al. 2018b)	3.00 ± 0.14	3.3	0.45 [†]	20	deep
DARTS (2nd order) (Liu et al. 2018b)	2.76 ± 0.09	3.3	1.50 [†]	20	deep
B-DARTS+CLR (1st order) (ours)	2.67 ± 0.12	3.3	0.09	8	broad
B-DARTS+CLR (2nd order) (ours)	2.80 ± 0.09	3.2	0.19	8	broad

[†] Obtained by DARTS using the code publicly released by the authors at <https://github.com/quark0/darts> on a single NVIDIA GTX 1080Ti GPU.

to 4 instead of 2 for DARTS. In the search phase of DARTS, there are more cells in the over-parameterized model than B-DARTS. Hence, DARTS needs more training data to optimize network parameters well.

4.3 Results on CIFAR-10

In B-DARTS, the over-parameterized model with broad topology consists of 3 cells (2 broad cells and 1 enhancement cell), where each one contains 2 input nodes, 4 intermediate nodes and 1 output node. For fair comparison of the proposed B-DARTS and vanilla DARTS, we also use almost all default hyper-parameters of DARTS (except batch size and learning rate) for B-DARTS. Benefit from the advantage of memory efficiency, larger batch size of 256 and learning rate of 0.1 than DARTS are used in the search phase of B-DARTS, respectively. Detailed experimental settings can be found in **Supplementary Material**. We visualize the best performing architectures learned by B-DARTS with CLR in Figure 4. Table 3 summaries the results of B-DARTS with CLR, and the comparison with vanilla DARTS.

The proposed B-DARTS takes full advantages of broad scalable architecture, so that great efficiency improvement can be obtained. For first order approximation, B-DARTS delivers state-of-the-art efficiency of 0.09 GPU day which is 5x faster than vanilla DARTS. Furthermore, B-DARTS achieves 7.9x (0.19 GPU day) less search cost than vanilla DARTS with second order approximation. From the point of view of accuracy, B-DARTS with CLR achieves 0.33% better performance compared with DARTS using first order approximation. Moreover, all learned broad scalable architec-

tures achieve competitive even better performance just using 8 cells, instead of 20 used in DARTS. This characteristic implies that the architecture learned by B-DARTS excels in obtaining faster training and inference speed than DARTS for real-world applications, e.g. mobile devices.

4.4 Results on ImageNet

In this section, only the best performing architecture learned by B-DARTS (1st order) with CLR is transferred to ImageNet, due to the restriction of computational resources. In previous works using deep scalable architecture, the learned architecture is transferred to ImageNet by the following way. Three 3×3 convolutions with stride 2 are treat as the stem layers for reducing the resolution of input images from 224×224 to 28×28 . Subsequently, the architecture learned on CIFAR-10 can be employed for image classification on ImageNet. Similarly, we leverage this way for the proposed approach named as B-DARTS-C2, i.e. using 2 convolution blocks to construct the ImageNet classifier. Beyond that, another way for broad model construction can be adopted. As aforementioned in Section 3.2, the number of convolution block is determined by the input size of first convolution block, which is similar to the number of reduction cell in deep scalable architecture. Consequently, we also employ 5 convolution blocks to construct the ImageNet classifier named B-DARTS-C5, for achieving possible better performance with full-scale representations. For B-DARTS-C2, we set both the number of deep cell in each convolution block and enhancement cell to 2. For B-DARTS-C5, there are 11 cells (1 deep cell and 1 broad cell in each convolution

Table 2: Comparison of our approach with other state-of-the-art image classifiers on ImageNet

Architecture	Test Err. (%)		Params (M)	Search Cost (GPU days)	Mult-Adds (M)	Topology
	top-1	top-5				
Inception-v1 (Szegedy et al. 2015)	30.2	10.1	6.6	-	1448	deep
MobileNet (Howard et al. 2017)	29.4	10.5	4.2	-	569	deep
ShuffleNet (Zhang et al. 2018)	26.4	10.2	~ 5	-	524	deep
AmoebaNet-A (Real et al. 2019)	25.5	8.0	5.1	3150	555	deep
AmoebaNet-B (Real et al. 2019)	26.0	8.5	5.3	3150	555	deep
AmoebaNet-C (Real et al. 2019)	24.3	7.6	6.4	3150	570	deep
NASNet-A (Zoph et al. 2018)	26.0	8.4	5.3	1800	564	deep
NASNet-B (Zoph et al. 2018)	27.2	8.7	5.3	1800	488	deep
NASNet-C (Zoph et al. 2018)	27.5	9.0	4.9	1800	558	deep
PNAS (Liu et al. 2018a)	25.8	8.1	5.1	225	588	deep
DARTS (2nd order) (Liu et al. 2018b)	26.7	8.7	4.7	1.50	574	deep
ProxylessNAS (GPU) (Cai et al. 2018)	24.9	7.5	7.1	8.30	465	deep
SNAS (mild) (Xie et al. 2018)	27.3	9.2	4.3	1.50	522	deep
P-DARTS (CIFAR-10) (Chen et al. 2019)	24.4	7.4	4.9	0.30	557	deep
P-DARTS (CIFAR-100) (Chen et al. 2019)	24.7	7.5	5.1	0.30	577	deep
PC-DARTS (CIFAR-10) (Xu et al. 2019)	25.1	7.8	5.3	0.10	586	deep
B-DARTS-C2 (1st order) (ours)	27.3	9.0	4.4	0.09	441	broad
B-DARTS-C5 (1st order) (ours)	27.2	9.0	3.7	0.09	938	broad

block, and 1 enhancement cell in each enhancement block) in the network. More experimental details can be found in **Supplementary Material**. We show the results in Table 4.

Obviously, both two classifiers achieve competitive performance in terms of test error. Moreover, B-DARTS-C5 achieves better accuracy than B-DARTS-C2 using less parameters. The above result implies that the strategy of multi-scale feature fusion contributes to the performance improvement of broad scalable architecture. Furthermore, the index of Mult-Adds of B-DARTS-C2 is state-of-the-art. However, B-DARTS-C5 has the largest index of Mult-Adds in Table 4 which does not satisfy the mobile setting (i.e. smaller than 600M), in spite of its index of parameters is just 3.7M. Here, the first three convolution blocks where the size of input is too large, lead to the above catastrophic phenomenon.

4.5 Effectiveness of Confident Learning Rate

To some extent, the number of convolutions in two types of cells, γ , is basically proportional to the accuracy of model (Guo et al. 2020), so that we employ γ as the index to examine the effectiveness of CLR for both B-DARTS and vanilla DARTS. Furthermore, we choose warmup strategy as the comparative method to further verify the effectiveness of CLR. We repeat running six methods (i.e. vanilla B-DARTS/DARTS, B-DARTS/DARTS with warmup, and B-DARTS/DARTS with CLR) for four times, and show the number of convolutions of entire search process in Figure 5.

For vanilla B-DARTS, the mean value of γ is about 3 which tends to deliver poor performance. Moreover, we train the architecture of case 2 learned by vanilla B-DARTS for 600 epochs. The architecture achieves 3.26% test error with 3.6M parameters under default hyper-parameters of DARTS. The warmup strategy contributes to the collapse issue mitigation of B-DARTS in terms of γ , where the mean

value of γ is about 4.5. For the proposed CLR, γ of four repeated implementations are 6, 8, 5, 5 (i.e. the sum of convolutions in both convolution and enhancement cells), respectively. Obviously, there are more convolutions in the learned cells by B-DARTS with CLR than warmup. Moreover, we also train the architecture of case 1 learned by B-DARTS using CLR for 600 epochs. The architecture achieves 2.90% test error with 3.4M parameters under the above setting for architecture evaluation.

From the overall perspective, γ for B-DARTS with CLR decreases firstly, and then increases to a high value. In the decreasing phase of γ , those weight-free operations are prone to be equipped with larger weights than the weight-equipped one, although the confident learning rate is small enough. The reason for above situation is that the outputs of weight-free operations are more consistent with its input, which is preferred by gradient-based search algorithm (Xu et al. 2019). With the convergence of over-parameterized model, the increasing phase of γ begins. Those well-optimized weight-equipped operations contribute to the improvement of validation accuracy, so that the search strategy starts to prefer them.

For vanilla DARTS, the mean value of γ is about 5, and only first implementation learns to utilize a convolutional operation in reduction cell. Here, a convolution in reduction cell tends to achieve satisfactory performance with larger probability than those cells consisted of all weight-free operations. Beyond that, DARTS with warmup delivers equal or worse performance than vanilla DARTS in terms of the number of convolutional operations. Moreover, it can not learn to employ convolutional operation in reduction cell for possible improvement. DARTS with CLR learns 6, 5, 8, 4 convolutions under four repeated implementations, whose mean value is about 6 (1 larger than vanilla DARTS). Importantly,

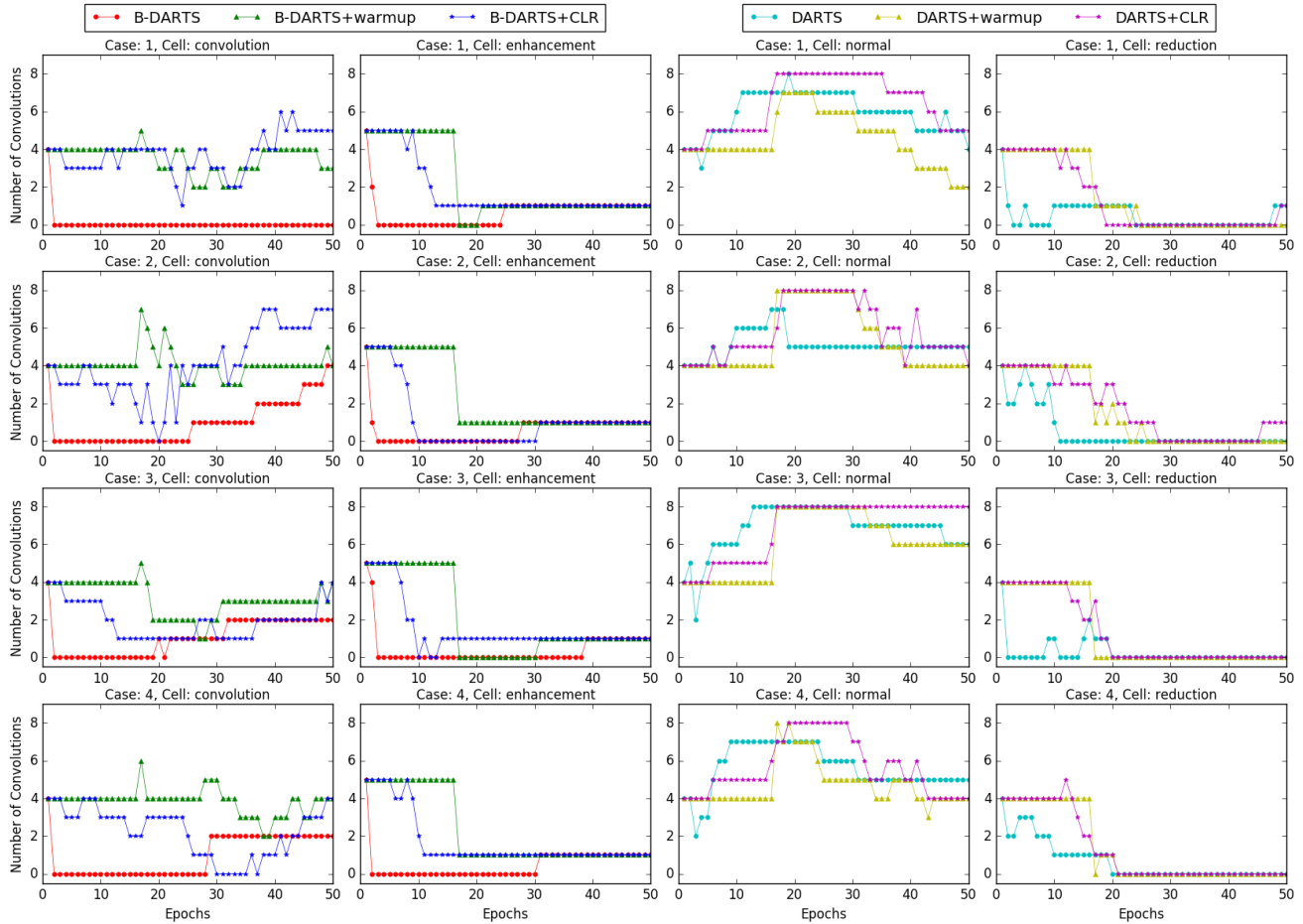


Figure 5: The number of convolutions of entire search process in two cells learned by B-DARTS, B-DARTS with warmup, B-DARTS with CLR, DARTS, DARTS with warmup, and DARTS with CLR under four repeated implementations. We use the sum of the number of convolution operations with regard to two cells as the index for performance evaluation.

the proposed CLR excels in discovering the reduction cell of DARTS with convolutional operation.

Above all, the proposed CLR is effective to solve the performance collapse issue for both B-DARTS and DARTS. Moreover, the value of confidence factor β should be determined by the depth of used over-parameterized model in architecture search phase, i.e. those deep scalable architectures should be equipped with larger value of β than the broad one, for training the over-parameterized model well.

4.6 B-PC-DARTS: Combining PC-DARTS with Broad Scalable Architecture

To further improve the efficiency of NAS, we also propose B-PC-DARTS, the combination of broad scalable architecture and PC-DARTS (Xu et al. 2019) whose efficiency is state-of-the-art (0.10 GPU day). For architecture search on CIFAR-10, the proposed B-PC-DARTS delivers 2x (0.05 GPU day) faster search efficiency than vanilla PC-DARTS. Moreover, vanilla PC-DARTS suffers from the out of memory (OOM) issue when using second order approximation with default batch size 256 on a single NVIDIA

GTX 1080Ti GPU. The reason is that there is no memory to construct an extra model for second order approximation in PC-DARTS (using about 12G memory with batch size 256). However, B-PC-DARTS does not suffer from the above OOM issue, due to enough memory is available for new model construction even though using batch size 512 for architecture search. Beyond that, B-PC-DARTS also achieves state-of-the-art efficiency of 0.19 GPU day¹ for proxyless search on ImageNet. We give experimental details and results about B-PC-DARTS in **Supplementary Material**.

5 Conclusions

In this paper, we propose B-DARTS to improve the efficiency of DARTS further, and CLR to mitigate the performance collapse issue in both B-DARTS and DARTS. B-DARTS achieves state-of-the-art search efficiency of NAS, 0.09 day on CIFAR-10 using a single NVIDIA GTX 1080Ti

¹Based on PC-DARTS using the code publicly released by the authors at <https://github.com/yuhuixu1993/PC-DARTS> on a single NVIDIA Tesla V100 GPU.

GPU. Moreover, the proposed CLR contributes both B-DARTS and DARTS to learn more convolutions in two types of cells for performance improvement. However, B-DARTS does not always improve the efficiency without performance drop. We will utilize knowledge distillation (Heo et al. 2019a,b) to solve this issue in the future.

Acknowledgments

This work was supported by No. GJHZ1849 International Partnership Program of Chinese Academy of Sciences.

References

- Cai, H.; Zhu, L.; Han, S.; et al. 2018. ProxylessNAS: Direct neural architecture search on target task and hardware. In *International Conference on Learning Representations (ICLR)*.
- Chen, C. P.; and Liu, Z. 2017. Broad learning system: An effective and efficient incremental learning system without the need for deep architecture. *IEEE Transactions on Neural Networks and Learning Systems* 29(1): 10–24.
- Chen, C. P.; Liu, Z.; Feng, S.; et al. 2018a. Universal approximation capability of broad learning system and its structural variations. *IEEE Transactions on Neural Networks and Learning Systems* 30(4): 1191–1204.
- Chen, X.; Xie, L.; Wu, J.; and Tian, Q. 2019. Progressive differentiable architecture search: Bridging the depth gap between search and evaluation. In *Proceedings of the IEEE International Conference on Computer Vision (ECCV)*, 1294–1303.
- Chen, Y.; Gao, R.; Liu, F.; and Zhao, D. 2020. ModuleNet: Knowledge-inherited neural architecture search. *arXiv preprint arXiv:2004.05020*.
- Chen, Y.; Zhao, D.; Lv, L.; and Zhang, Q. 2018b. Multi-task learning for dangerous object detection in autonomous driving. *Information Sciences* 432: 559–571.
- Chu, X.; Zhang, B.; Xu, R.; and Li, J. 2019. Fairnas: Rethinking evaluation fairness of weight sharing neural architecture search. *arXiv preprint arXiv:1907.01845*.
- Devries, T.; and Taylor, G. W. 2017. Improved regularization of convolutional neural networks with cutout. *arXiv preprint arXiv:1708.04552*.
- Ding, Z.; Chen, Y.; Li, N.; Zhao, D.; Sun, Z.; and Chen, C. 2020. BNAS: An efficient neural architecture search approach using broad scalable architecture. *arXiv preprint arXiv:2001.06679v2*.
- Feng, S.; and Chen, C. P. 2018. Fuzzy broad learning system: A novel neuro-fuzzy model for regression and classification. *IEEE transactions on cybernetics* 50(2): 414–424.
- Guo, M.; Yang, Y.; Xu, R.; Liu, Z.; and Lin, D. 2020. When NAS meets robustness: In search of robust architectures against adversarial attacks. In *Proceedings of the IEEE Conference on Computer Vision and Pattern Recognition (CVPR)*, 631–640.
- He, K.; Zhang, X.; Ren, S.; and Sun, J. 2016. Deep residual learning for image recognition. In *Proceedings of the IEEE Conference on Computer Vision and Pattern Recognition (CVPR)*, 770–778.
- Heo, B.; Lee, M.; Yun, S.; and Choi, J. Y. 2019a. Knowledge distillation with adversarial samples supporting decision boundary. In *Proceedings of the AAAI Conference on Artificial Intelligence (AAAI)*, volume 33, 3779–3787.
- Heo, B.; Lee, M.; Yun, S.; and Choi, J. Y. 2019b. Knowledge transfer via distillation of activation boundaries formed by hidden neurons. In *Proceedings of the AAAI Conference on Artificial Intelligence (AAAI)*, volume 33, 3771–3778.
- Howard, A. G.; Zhu, M.; Chen, B.; Kalenichenko, D.; Wang, W.; Weyand, T.; Andreetto, M.; and Adam, H. 2017. Mobilenets: Efficient convolutional neural networks for mobile vision applications. *arXiv preprint arXiv:1704.04861*.
- Kingma, D.; and Ba, L. 2015. Adam: A method for stochastic optimization. In *International Conference on Learning Representations (ICLR)*.
- Krizhevsky, A.; and Hinton, G. 2009. Learning multiple layers of features from tiny images.
- Li, H.; Zhang, Q.; Zhao, D.; et al. 2020. Deep Reinforcement learning-based Automatic exploration for navigation in unknown environment. *IEEE Transactions on Neural Networks and Learning Systems* 31(6): 2064–2076.
- Liang, H.; Zhang, S.; Sun, J.; He, X.; Huang, W.; Zhuang, K.; and Li, Z. 2019. Darts+: Improved differentiable architecture search with early stopping. *arXiv preprint arXiv:1909.06035*.
- Liu, C.; Chen, L.-C.; Schroff, F.; Adam, H.; Hua, W.; Yuille, A. L.; and Fei-Fei, L. 2019. Auto-deeplab: Hierarchical neural architecture search for semantic image segmentation. In *Proceedings of the IEEE conference on Computer Vision and Pattern Recognition (CVPR)*, 82–92.
- Liu, C.; Zoph, B.; Neumann, M.; Shlens, J.; Hua, W.; Li, L.; Fei-Fei, L.; Yuille, A.; Huang, J.; and Murphy, K. 2018a. Progressive neural architecture search. In *Proceedings of the European Conference on Computer Vision (ECCV)*, 19–34.
- Liu, H.; Simonyan, K.; Yang, Y.; et al. 2018b. DARTS: Differentiable architecture search. In *International Conference on Learning Representations (ICLR)*.
- Loshchilov, I.; and Hutter, F. 2017. SGDR: Stochastic gradient descent with warm restarts. In *International Conference on Machine Learning (ICLR)*.
- Pham, H.; Guan, M.; Zoph, B.; Le, Q.; and Dean, J. 2018. Efficient neural architecture search via parameters sharing. In *International Conference on Machine Learning (ICLR)*, 4095–4104.
- Real, E.; Aggarwal, A.; Huang, Y.; and Le, Q. V. 2019. Regularized evolution for image classifier architecture search. In *Proceedings of the AAAI Conference on Artificial Intelligence (AAAI)*, volume 33, 4780–4789.
- Redmon, J.; Divvala, S.; Girshick, R.; and Farhadi, A. 2016. You only look once: Unified, real-time object detection. In

Proceedings of the IEEE conference on Computer Vision and Pattern Recognition (CVPR), 779–788.

Redmon, J.; and Farhadi, A. 2017. YOLO9000: Better, faster, stronger. In *Proceedings of the IEEE conference on Computer Vision and Pattern Recognition (CVPR)*, 7263–7271.

Redmon, J.; and Farhadi, A. 2018. Yolov3: An incremental improvement. *arXiv preprint arXiv:1804.02767*.

Russakovsky, O.; Deng, J.; Su, H.; Krause, J.; Satheesh, S.; Ma, S.; Huang, Z.; Karpathy, A.; Khosla, A.; Bernstein, M.; et al. 2015. Imagenet large scale visual recognition challenge. *International Journal of Computer Vision* 115(3): 211–252.

Shao, K.; Zhao, D.; Li, N.; and Zhu, Y. 2018. Learning battles in ViZDoom via deep reinforcement learning. In *2018 IEEE Conference on Computational Intelligence and Games (CIG)*, 1–4. IEEE.

Shao, K.; Zhu, Y.; Zhao, D.; et al. 2019. Starcraft micromanagement with reinforcement learning and curriculum transfer learning. *IEEE Transactions on Emerging Topics in Computational Intelligence* 3(1): 73–84.

Szegedy, C.; Liu, W.; Jia, Y.; Sermanet, P.; Reed, S.; Anguelov, D.; Erhan, D.; Vanhoucke, V.; and Rabinovich, A. 2015. Going deeper with convolutions. In *Proceedings of the IEEE Conference on Computer Vision and Pattern Recognition (CVPR)*, 1–9.

Vaswani, A.; Shazeer, N.; Parmar, N.; Uszkoreit, J.; Jones, L.; Gomez, A. N.; Kaiser, Ł.; and Polosukhin, I. 2017. Attention is all you need. In *Advances in Neural Information Processing Systems (NIPS)*, 5998–6008.

Williams, R. J. 1992. Simple statistical gradient-following algorithms for connectionist reinforcement learning. *Machine Learning* 8(3-4): 229–256.

Xie, S.; Zheng, H.; Liu, C.; and Lin, L. 2018. SNAS: stochastic neural architecture search. In *International Conference on Learning Representations (ICLR)*.

Xu, Y.; Xie, L.; Zhang, X.; Chen, X.; Qi, G.-J.; Tian, Q.; and Xiong, H. 2019. PC-DARTS: Partial channel connections for memory-efficient architecture search. In *International Conference on Learning Representations (ICLR)*.

Zhang, X.; Zhou, X.; Lin, M.; and Sun, J. 2018. Shufflenet: An extremely efficient convolutional neural network for mobile devices. In *Proceedings of the IEEE Conference on Computer Vision and Pattern Recognition (CVPR)*, 6848–6856.

Zhao, D.; Chen, Y.; Lv, L.; et al. 2017. Deep reinforcement learning with visual attention for vehicle classification. *IEEE Transactions on Cognitive and Developmental Systems* 9(4): 356–367.

Zoph, B.; and Le, Q. V. 2017. Neural architecture search with reinforcement learning. In *International Conference on Learning Representations (ICLR)*.

Zoph, B.; Vasudevan, V.; Shlens, J.; and Le, Q. V. 2018. Learning transferable architectures for scalable image recognition. In *Proceedings of the IEEE Conference on*

Computer Vision and Pattern Recognition (CVPR), 8697–8710.

Supplement

Differentiable Architecture Search Combining Broad Scalable Architecture with Partial Channel Connections

Preliminary: Differentiable Architecture Search with Partial Channel Connections Differentiable paradigm contributes DARTS (Liu et al. 2018b) to achieve fast search speed. However, the above pipeline is memory-inefficient. In PC-DARTS (Xu et al. 2019), the strategy of partial channel connections is adopted to address the above drawback. For the connection from $x_{(j)}$ to $x_{(i)}$, PC-DARTS feeds partial channels into $|\mathcal{O}|$ operations where \mathcal{O} represents the predefined space for candidate operations, and copies others to the output directly. Consequently, the continuous relaxation of PC-DARTS can be computed by

$$f_{(i,j)}^{PC}(x_{(j)}; M_{(i,j)}) = \sum_{o \in \mathcal{O}} \frac{\exp(\alpha_{(i,j)}^o)}{\sum_{o' \in \mathcal{O}} \exp(\alpha_{(i,j)}^{o'})} o(M_{(i,j)} * x_{(j)}) + (1 - M_{(i,j)}) * x_{(j)}, \quad (4)$$

where, $M_{(i,j)}$ denotes channels sampling mask whose values are chosen from 0 (masked channels) and 1 (selected channels), $M_{(i,j)} * x_{(j)}$ represents the chosen channels and $(1 - M_{(i,j)}) * x_{(j)}$ computes the masked one. Benefit from partial channel connection, the memory usage of gradient-based pipeline is reduced greatly, so that larger batch size can be set and higher efficiency can be achieved compared with vanilla DARTS.

B-PC-DARTS Similar to B-DARTS, the proposed B-PC-DARTS treats Broad Convolutional Neural Network (BCNN) as the broad scalable architecture for search. Furthermore, B-PC-DARTS is able to obtain faster search efficiency than B-DARTS. On one hand, PC-DARTS is also a gradient-based NAS pipeline so that full advantages of BCNN can be taken. On the other hand, the strategy of partial channel connections is employed. The above strategy does not only contribute to the search efficiency improvement, but also relieve the performance collapse issue (Liang et al. 2019; Xu et al. 2019) of vanilla DARTS. As a result, the proposed Confident Learning Rate (CLR) is not employed in B-PC-DARTS, and \mathcal{O} for the proposed B-PC-DARTS contains 8 candidate operations, i.e. *separable convolution* with 3×3 and 5×5 kernels, *dilated separable convolution* with 3×3 and 5×5 kernels, *max pooling* and *average pooling* with 3×3 kernel, *skip connection*, and *zero (none)*.

Experimental Details on CIFAR-10

Dataset There are 60K images with spatial resolution of 32×32 in CIFAR-10 (Krizhevsky and Hinton 2009), where 50K for training and 10K for test. A list of standard methods are applied for preprocessing of CIFAR-10, e.g. randomly flipping and cropping.

Table 3: Comparison of the proposed B-PC-DARTS and vanilla PC-DARTS on CIFAR-10.

Architecture	Error (%)	Params (M)	Search Cost (GPU days)	Number of Cells	Topology
PC-DARTS (1st order) (Xu et al. 2019)	2.57 \pm 0.07	3.6	0.10	20	deep
PC-DARTS (2nd order) (Xu et al. 2019)	-	-	OOM [†]	-	-
B-PC-DARTS (1st order) (ours)	2.79 \pm 0.19	3.7	0.05	8	broad
B-PC-DARTS (2nd order) (ours)	2.77 \pm 0.09	3.5	0.09	8	broad

[†] Obtained by PC-DARTS using the code publicly released by the authors at <https://github.com/yuhuixu1993/PC-DARTS> with default setting for first order approximation of batch size 256 on a single NVIDIA GTX 1080Ti GPU.

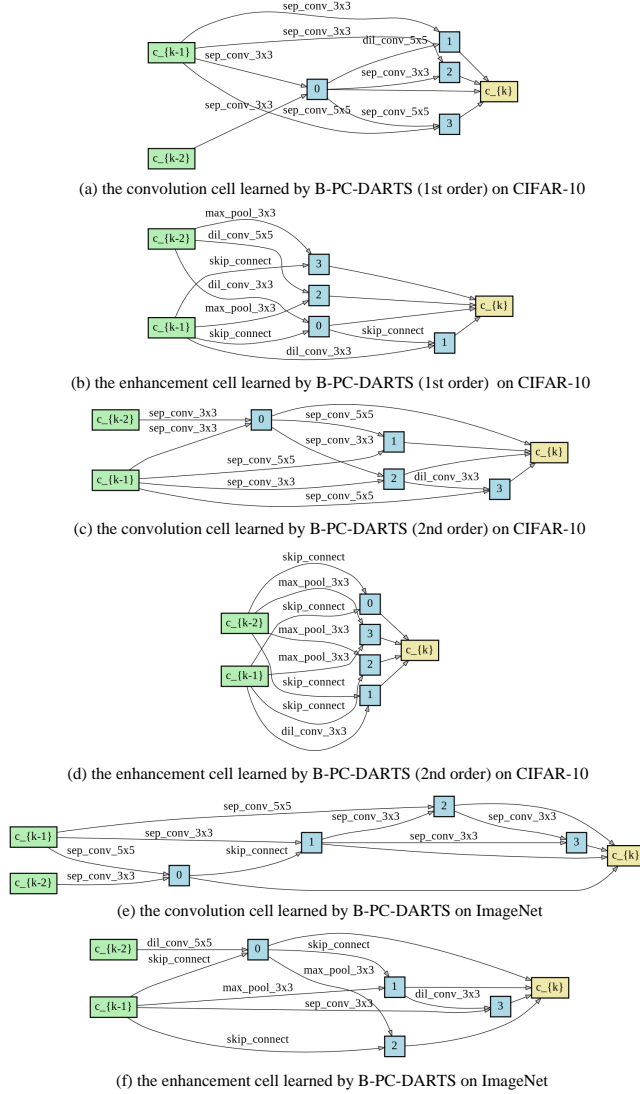


Figure 6: The architectures learned by B-PC-DARTS on CIFAR-10 and ImageNet.

Experimental Setting for Search Phase In the architecture search phases of B-DARTS and B-PC-DARTS, there are many identical experimental details as below. We set the number of initial input channels to 16 and train the broad

over-parameterized model for 50 epochs. The split portion of proxy dataset is set to 0.5, i.e. two subsets, each one with 25K training data of CIFAR-10, that are used for training the broad over-parameterized model and architecture weights, respectively. The SGD optimizer (Loshchilov and Hutter 2017) is employed to learn the broad network weights, with dynamic learning rate (annealed down to zero following a cosine schedule without restart), momentum 0.9, weight decay 3×10^{-4} . For architecture weights, we use zero initialization to generate α for both convolution and enhancement cells. Moreover, we utilize Adam (Kingma and Ba 2015) with momentum (0.5, 0.999) and weight decay 10^{-3} , as the optimizer to update α . We run four repeated experiments of architecture search for B-DARTS and B-PC-DARTS, and choose the best performing architecture as the optimal one. There are also some differences between the experimental settings of B-DARTS and B-PC-DARTS as below.

On one hand, the learning rate of architecture weights η_α is set to 3×10^{-4} in B-DARTS. Moreover, we employ CLR with $\beta = 2$ to mitigate the performance collapse issue of B-DARTS. On the other hand, η_α used for B-PC-DARTS is set to 6×10^{-4} . The strategy of partial channel connections contributes PC-DARTS to discover novel architecture with batch size 256 and learning rate 0.1. Furthermore, B-PC-DARTS can use batch size 512 with learning rate 0.2 for architecture search due to the contribution of memory efficiency. The combination of warmup strategy and partial channel connection is also adopted to alleviate the performance collapse issue of broad over-parameterized model. The architectures learned by B-PC-DARTS on CIFAR-10 are visualized in Figure 6 (a) to (d).

Experimental Setting for Evaluation Phase For the architecture evaluation stage, B-DARTS and B-PC-DARTS use identical experimental settings as follows. The model is constructed by stacking 8 cells (2 deep cells and 1 broad cell in each convolution block, and 2 enhancement cells). We tune the number of initial input channels to fit the parameters following a mobile setting between 3~4M. Furthermore, the model is trained for 2000 epochs using SGD optimizer with batch size 128, initial learning rate 0.025 (the decayed way following the search phase), momentum 0.9, weight decay 3×10^{-4} . Moreover, cutout with 16 length (Devries and Taylor 2017) and drop path with a probability of 0.3 are adopted. The experimental results (*mean* \pm *std*) are obtained by three repeated experiments and shown in Table 3.

Table 4: Comparison of the proposed B-PC-DARTS and vanilla PC-DARTS on ImageNet

Architecture	Test Err. (%)		Params (M)	Search Cost (GPU days)	Mult-Adds (M)	Topology
	top-1	top-5				
PC-DARTS (CIFAR-10)(Xu et al. 2019)	25.1	7.8	5.3	0.10	586	deep
PC-DARTS (ImageNet) (Xu et al. 2019) [†]	24.2	7.3	5.3	0.45 [‡]	597	deep
B-PC-DARTS-C2 (2nd order) (CIFAR-10) (ours)	27.2	8.8	4.6	0.09	475	broad
B-PC-DARTS-C2 (ImageNet) (ours) [†]	27.0	10.5	4.6	0.19	576	broad

[†] Those architectures are discovered on ImageNet directly.

[‡] Obtained by PC-DARTS using the code publicly released by the authors at <https://github.com/yuhuixu1993/PC-DARTS> on a single NVIDIA Tesla V100 GPU.

Analysis for B-PC-DARTS Compared with the baseline of PC-DARTS, B-PC-DARTS achieves state-of-the-art efficiency, 2x less computational cost (about 70 minutes) by using first order approximation. Beyond that, B-PC-DARTS obtains competitive 2.79 ± 0.19 test error with 3.7M parameters. In particular, PC-DARTS suffers from the Out of Memory (OOM) issue when using second order approximation with batch size 256 on a single NVIDIA GTX 1080Ti GPU. The reason is that there are no memory to construct an extra model for second order approximation in PC-DARTS (using about 12G memory with batch size 256). However, B-PC-DARTS does not suffer from the above OOM issue, due to enough memory is available for new model construction even though using batch size 512 for architecture search.

Experimental Details on ImageNet

Dataset ImageNet (Russakovsky et al. 2015) is a popular dataset for large scale image classification task. There are about 1.3M images with various spatial resolution in ImageNet, that are near equally distributed over 1000 object categories. Similarly, a series of data preprocessing techniques are applied to ImageNet, e.g. randomly flipping and cropping. Following previous works (Zoph et al. 2018; Liu et al. 2018b; Chen et al. 2019; Xie et al. 2018; Liang et al. 2019; Xu et al. 2019), we reshape the size of original images of ImageNet to 224×224 .

Experimental Setting for B-DARTS We only transfer the best performing architecture learned by B-DARTS (1st order) for solving large image classification task on ImageNet. Furthermore, there are two types of paradigms, as aforementioned B-DARTS-C2 (i.e. including 2 convolution blocks) and B-DARTS-C5 (i.e. including 5 convolution blocks), for classifier construction. For B-DARTS-C2, we set both the number of deep cell in each convolution block and enhancement cell to 2. For B-DARTS-C5, there are 11 cells (1 deep cell and 1 broad cell in each convolution block, and 1 enhancement cell in each enhancement block) in the network. In the architecture evaluation phase of B-DARTS-C5 on ImageNet, we train the architecture for 150 epochs with batch size 768 using 8 NVIDIA Tesla V100 GPUs. We also choose SGD as the optimizer with initial learning rate 0.1 (decayed by a factor of 0.1 at 80-th, 120-th and 140-th epoch), momentum 0.9 and weight decay 3×10^{-5} . Moreover, the initial input channels of B-DARTS-C5 are set to 6, the label smoothing is set to 0.1, and the gradient clip bound is set

to 5.0. Due to the topology difference, B-DARTS-C2 can set larger batch size and learning rate than B-DARTS-C5 for model training on ImageNet. Consequently, we leverage various hyper-parameters from B-DARTS-C5 with respect to batch size, the initial value and decayed way of learning rate for B-DARTS-C2 as follows. We train B-DARTS-C2 for 250 epochs with batch size 1024 using 2 NVIDIA Tesla V100 GPUs. Similarly, we also choose the SGD optimizer with initial learning rate 0.5 whose decayed way is identical with PC-DARTS (Xu et al. 2019) used on ImageNet training. Moreover, the initial input channels of B-DARTS-C2 are set to 48.

Experimental Setting for B-PC-DARTS For B-PC-DARTS, we not only transfer the architecture learned on CIFAR-10 to ImageNet, but also directly search architecture on ImageNet rather than using proxy dataset. For architecture transfer, only the architecture learned by B-PC-DARTS (2nd order) is stacked for large scale image classification using 2 convolution blocks, due to the restriction of computational resources. The used hyper-parameters are identical with B-DARTS-C2. Beyond that, we employ B-PC-DARTS to directly search architecture on ImageNet, and use the learned architecture for large scale image classification. Moreover, two subsets contained 10% and 2.5% of 1.3 millions images, are randomly sampled from each category of training data of ImageNet for broad over-parameterized model and architecture weights training, respectively. Similar to the search phase of PC-DARTS on ImageNet, we treat three 3×3 convolutions with stride 2 as stem layers for reducing the resolution of input images from 224×224 to 28×28 . Subsequently, the broad over-parameterized model used on CIFAR-10 can be employed for proxyless architecture search on ImageNet. Here, we use a single Tesla V100 GPU for search, and set the batch size and learning rate to 512 and 0.2, respectively. Other hyper-parameters are similar to B-PC-DARTS used for search on CIFAR-10. For the architecture directly learned on ImageNet, we construct the classifier with 2 convolution blocks by stacking 10 cells (3 deep cells in each convolution block, and a single enhancement block). Moreover, the initial input channels of B-DARTS-C2 are set to 50. Similarly, we visualize the convolution and enhancement cells learned by B-PC-DARTS on ImageNet in Figure 6 (e) and (f) respectively, and summary the comparison of B-PC-DARTS and vanilla PC-DARTS on ImageNet in Table 4.

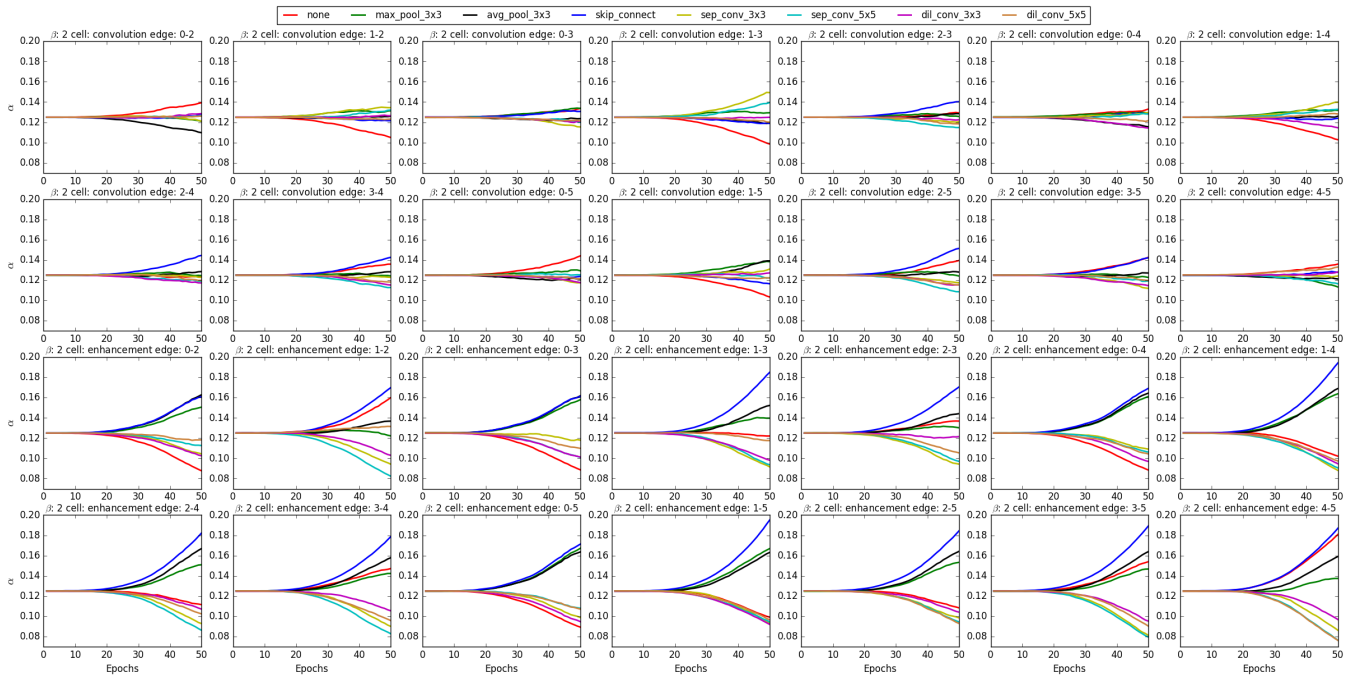


Figure 7: Performance collapse issue of convolution (subgraph 1 to 14) and enhancement (subgraph 15 to 28) cells in B-DARTS when employing *skip connection* in search space \mathcal{O} .

Analysis for B-PC-DARTS B-PC-DARTS also delivers state-of-the-art search efficiency for proxyless architecture search on ImageNet. The entire search process spends around 4.6 hours (about 2.4x faster than vanilla PC-DARTS) on a single NVIDIA Tesla V100 GPU. In addition, the indices of parameters and Mult-Adds of both two architectures learned by B-PC-DARTS are better than vanilla PC-DARTS, especially for the later one. Beyond that, all broad architectures achieve competitive accuracy just using few parameters, that is contributed by the multi-scale feature fusion of broad scalable architecture. Moreover, the architecture directly learned on ImageNet outperforms the one learned on proxy data in terms of the top-1 accuracy. This indicates that the proposed B-PC-DARTS is effective for proxyless architecture search on ImageNet.

Admittedly, there exists a relative large performance gap for ImageNet classification between B-PC-DARTS and PC-DARTS, i.e. broad and deep scalable architectures. Due to the restriction of computational resources, we can not determine a list of appropriate hyper-parameters for the learned broad architectures, e.g. the number of deep and enhancement cells. Beyond that, we argue that the number of convolution blocks maybe plays an important role for broad deep scalable architecture in ImageNet classification task. This is similar to the backbone design of YOLOv3 (Redmon and Farhadi 2018), which obtains better detection performance using multi-scale prediction, i.e. feature maps with the sizes of 32×32 , 16×16 , and 8×8 , than previous versions of YOLO (Redmon et al. 2016; Redmon and Farhadi 2017). As a result, the optimal list of hyper-parameters including the number of convolution blocks, needs to be determined

further through intensive experiments for large scale image classification. We believe that the above performance gap can be bridged with an optimal list of appropriate hyper-parameters in the future.

The Reason to Remove Skip Connection for B-DARTS

In the architecture search phase of B-DARTS, we remove the *skip connection* from search space \mathcal{O} , due to it is predominant for almost all edges of enhancement cell in spite of using the proposed CLR. We visualize the architecture weights with respect to each edge of convolution and enhancement cells in Figure 7. Obviously, the proposed CLR can not make the *skip connection* (i.e. the blue line) out of predominance, especially for the enhancement cell. Moreover, full *skip connection*-consisted enhancement cell dose not work for broad scalable architecture. As described in DARTS+ (Liang et al. 2019), the first cell employs fresh images as input and the input of last one is mixed with a great number of noise, so that enhancement cell suffers from the collapse issue worse than the convolutional one. From above, we remove *skip connection* from search space \mathcal{O} for B-DARTS. Moreover, we will try to solve this issue in the future work.